scientific reports

Check for updates

OPEN

Bacteriophage Indie resensitizes multidrug-resistant *Acinetobacter baumannii* to antibiotics *in vitro*

Alma Karen Orozco-Ochoa[1], Jean Pierre González-Gómez[1], Beatriz Quiñones[2], Nohelia Castro-del Campo[1], José Benigno Valdez-Torres[1] & Cristóbal Chaidez-Quiroz[1]✉

Antimicrobial resistance in *Acinetobacter baumannii* poses a significant global health challenge. Phage therapy, particularly through phage-antibiotic synergy (PAS), offers a promising strategy to combat this pathogen. This study demonstrated significant PAS, where the combination of phage Indie and ceftazidime achieved a bacterial reduction of more than 85% of *A. baumannii* strain AbAK03 at 17 h using low doses. Notably, this combination overcame phage resistance observed at 4 h when the phage was used alone, extending bacterial eradication by 13 h. Furthermore, phage Indie restored bacterial susceptibility to ceftazidime, supporting its role in improving interventional treatments against multidrug-resistant *A. baumannii*. To explore this interaction, phage Indie was isolated and characterized from multidrug-resistant clinical strains. An *in vitro* PAS experiment was performed using ceftazidime and piperacillin-tazobactam. The combination of phage Indie with ceftazidime consistently showed superior bactericidal effects compared to either agent alone, while the combination of phage Indie with piperacillin-tazobactam exhibited an antagonistic effect. These findings provide clear evidence supporting the application of phage-antibiotic combinations as an effective intervention strategy and lay the groundwork for future *in vivo* trials in a mouse model to combat antimicrobial resistance.

Keywords *Acinetobacter baumannii*, Antimicrobial resistance, Phage-resistance, *In vitro* phage-antibiotic synergy, Restoring antibiotic efficacy, Phage therapy

Antimicrobial resistance (AMR) is a growing global threat, recognized as one of the top 10 public health risks[1]. The widespread use of antibiotics has exacerbated the crisis, increasing reliance on combination therapies[2]. The COVID-19 pandemic likely worsened AMR through inappropriate antibiotic use, fueling multidrug-resistant infections[3]. Despite mitigation efforts, horizontal gene transfer drives the emergence of multidrug-resistant (MDR), extensively drug-resistant (XDR), and pan-drug-resistant pathogens[4]. If left unaddressed, AMR could cause 10 million premature deaths annually by 2050[5], with an additional 100 billion dollars in healthcare costs[6]. The ESKAPE pathogens (*Enterococcus faecium*, *Enterococcus faecalis*, *Staphylococcus aureus*, *Klebsiella pneumoniae*, *Acinetobacter baumannii*, *Pseudomonas aeruginosa*, *Enterobacter* spp.) continue to evade most antimicrobials, causing the majority of hospital-acquired infections[7].

Acinetobacter baumannii, a Gram-negative coccobacillus, presents a significant challenge in hospitals due to limited treatment options[8]. This pathogen primarily affects immunocompromised patients in intensive care units (ICUs), leading to pneumonia, urinary tract infections, and bacteremia[9]. *A. baumannii*'s resistance, particularly through β-lactamases and antimicrobial-inactivating enzymes[9], and its virulence, linked to iron acquisition, biofilm formation, motility, and genetic adaptation, enable cell adhesion and tissue damage[10]. The capsule aids in biofilm formation and resistance to desiccation, disinfectants, and antibiotics[11]. Outbreaks of *A. baumannii* have surged globally[12–14], with carbapenem-resistant strains now classified as a top priority for treatment[15]. In the United States, 9,000 cases were reported annually from 2012 to 2017[16]. In Mexico, *A. baumannii* ranked fourth among isolated pathogens in 2023, with 550 healthcare-associated infections[17]. Specifically, in the state of Sinaloa in Northwestern Mexico, *A. baumannii* was identified as the fourth most common causative agent in primary healthcare infections, comprising 4.24% of total reported cases in December 2023[18].

[1]Centro de Investigación en Alimentación y Desarrollo, A.C. (CIAD), Laboratorio Nacional para la Investigación en Inocuidad Alimentaria (LANIIA), Carretera a Eldorado Km 5.5, Campo El Diez, 80110 Culiacan, Sinaloa, Mexico. [2]U.S. Department of Agriculture, Agricultural Research Service, Western Regional Research Center, Produce Safety and Microbiology Research Unit, Albany, CA 94710, USA. ✉email: chaqui@ciad.mx

Novel intervention alternatives are urgently needed to combat *A. baumannii*, a high-priority pathogen[15]. Bacteriophages, naturally occurring viruses, target specific bacteria and are abundant predators in nature[19]. Their ability to target bacterial strains, disrupt biofilms, and maintain low toxicity makes them an attractive option for bacterial eradication[20].

Phage therapy offers a promising alternative against MDR *A. baumannii* and AMR, with positive results in laboratories, animal models, and clinical cases, both alone and combined with other phages[21,22]. For example, phage Phab24 effectively targeted colistin-resistant *A. baumannii*, highlighting the need for further evaluation of phage stability, infection dynamics, and genomic safety[23]. A nine-phage cocktail successfully treated a 68-year-old diabetic with necrotizing pancreatitis and MDR *A. baumannii*, demonstrating the potential of phage therapy[20]. Additionally, combining phages with antibiotics has emerged as a promising strategy to enhance antibacterial activity, a phenomenon known as phage-antibiotic synergy (PAS)[24,25]. *In vitro* studies show that phage-antibiotic combinations provide superior bactericidal effects against *A. baumannii* compared to either agent alone, driving bacterial evolution toward phage resistance while resensitizing bacteria to antibiotics[26–29]. For instance, the combination of phage ΦFG02 and ceftazidime has shown significant synergy ($P = 0.001$) in eliminating *A. baumannii*[30]. Moreover, combining phage pB3074 with cefotaxime and meropenem effectively eradicated biofilms and treated wound infections in a pig skin model[28].

This study highlights the potential of the novel lytic bacteriophage vB_AbaP_Indie as a promising strategy to address AMR. The phage exhibits favorable biological and genomic properties and shows promise against MDR *A. baumannii*. The research aims to expand a local phage library targeting this pathogen and explore the synergy between phage vB_AbaP_Indie and two β-lactam antibiotics to enhance bacterial eradication. These findings highlight the importance of combining phages with antibiotics to overcome resistance and promote the development of alternative antimicrobial strategies. Furthermore, the availability of a well-characterized phage library tailored to local clinical isolates addresses a key limitation of phage therapy, enabling potential advances in *in vivo* trials and compassionate use in Mexico. These efforts could improve clinical outcomes and foster broader adoption of phage therapy.

Results

Bacterial strains identification

The susceptibility of ten *A. baumannii* strains and thirteen ESKAPE pathogens (*E. faecalis*, *S. aureus*, *K. pneumoniae*, and *P. aeruginosa*) and two Gram-negative pathogens (*E. coli*), as well as the ceftazidime and piperacillin-tazobactam MIC values for *A. baumannii* strain AbAK03, were interpreted following Clinical and Laboratory Standards Institute (CLSI) protocols (Table 1). The multiresistance of the bacterial isolates is corroborated with the zone of inhibition using the Kirby-Bauer disk diffusion test (Fig. S1). Specifically, *A. baumannii* strain AbAK03, the host bacterium of phage Indie, exhibited resistance to ceftazidime but susceptibility to piperacillin-tazobactam. The species was confirmed by PCR $bla_{\text{OXA-51}}$ for AbAK03 (Fig. S2).

Isolation and characterization of phage *Acinetobacter baumannii* phage vB_AbaP_Indie

Eight samples from wastewater treatment plants were obtained and analyzed to identify phages with lytic activity against clinical strains of MDR *A. baumannii*. One phage was isolated using a clinical strain AbAK03 as the host bacterium. In accordance with the guidance provided by the Bacterial and Archaeal Viruses Subcommittee of the International Committee on Taxonomy of Viruses (ICTV)[31], it was designated as *Acinetobacter baumannii* phage vB_AbaP_Indie, or just phage Indie, as its common name. Phage Indie, produced small, clear, uniform, round plaques with average size with a range of size 2 mm in diameter on *A. baumannii* strain AbAK03 lawn (Fig. 1A). The small plaques exhibited a clear halo around them with a range of size ~ 3 and 4 mm in diameter. The translucent halos were attributed to the action of depolymerase, an enzyme capable of breaking down bacterial surface polysaccharides[32]. Plaque assays showed that the purified phage reached a titer of 4.1×10^8 Plaque Forming Units (PFU) per mL. Transmission electron microscopy revealed the structure of phage Indie, displaying an icosahedral capsid and a short tail, typical of the abolished *Podoviridae* family (Fig. 1B).

Antibiotic		*Acinetobacter baumannii* strain									
		AbAK01	AbAK02	AbAK03	AbAK04	AbAK05	AbAK06	AbAK07	AbAK08	AbAK09	AbAK10
Ceftazidime (CFZ)	Sensitivity	R	S	R	S	S	S	S	S	S	S
	MIC[a] (μg/mL)	> 32	0.2	> 32	0.2	4	4	4	4	1.6	4
		> 32	0.2	> 32	0.4	4	4	4	8	1.6	4
		> 32	0.4	> 32	0.2	4	4	4	4	3.2	4
Piperacillin-tazobactam (TZP)	Sensitivity	S	S	S	S	S	S	S	S	S	S
	MIC[a] (μg/mL)	8/3.2	4/0.8	8/3.2	8/4	16/4	16/4	16/4	4/1.6	4/1.6	4/1.6
		8/3.2	4/0.4	8/3.2	8/4	8/4	16/4	16/4	8/3.2	4/1.6	4/1.6
		8/3.2	4/0.8	8/3.2	8/4	8/4	16/4	16/4	4/1.6	4/1.6	4/1.6

Table 1. Antibiotic sensitivity pattern of *A. baumannii*. [a]MIC, Minimum Inhibitory Concentration; Sensitivity: I, intermediate susceptibility; R, resistant; S, susceptible.

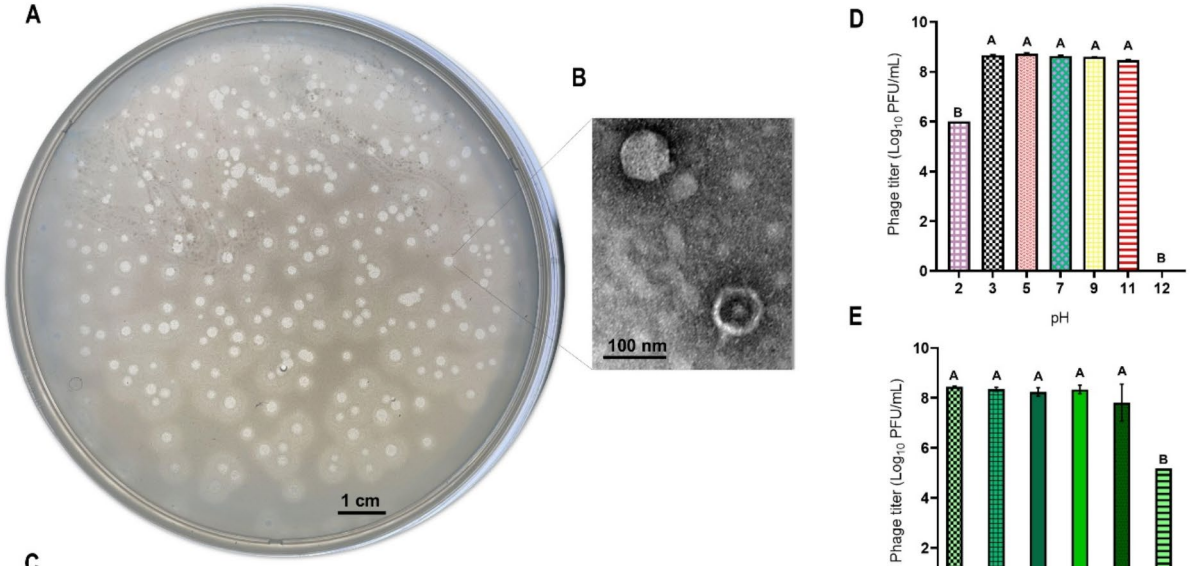

C

Phage Host Range		
Pathogens	**Ref.**	**Indie**
A. baumannii	AbAK01	(1)H
A. baumannii	AbAK02	
A. baumannii	AbAK03	(0.9)H
A. baumannii	AbAK04	
A. baumannii	AbAK05	
A. baumannii	AbAK06	
A. baumannii	AbAK07	
A. baumannii	AbAK08	
A. baumannii	AbAK09	
A. baumannii	AbAK10	
P. aeruginosa	PaAK07	
P. aeruginosa	PaAK08	
P. aeruginosa	PaAK10	
P. aeruginosa	PaAK11	
E. faecalis	EfAK11	
K. pneumoniae	KpAK11	
K. pneumoniae	KpAK13	
K. pneumoniae	KpAK14	(1)H
K. pneumoniae	KpAK15	
K. pneumoniae	KpAK16	
K. pneumoniae	KpAK17	
K. pneumoniae	KpAK18	
S. aureus	SaAK16	
E. coli	EcoAK05	
E. coli	EcoAK06	

Productive infection (EOP %)
No lysis
Partial lysis
Nebula lysis
Phage resistance

Plate efficiency (EOP):
H high (EOP ≥0.5)
M medium (0.1≤EOP<0.5)
L low (0.001<EOP<0.1)
I ineffective (EOP≤0.001)

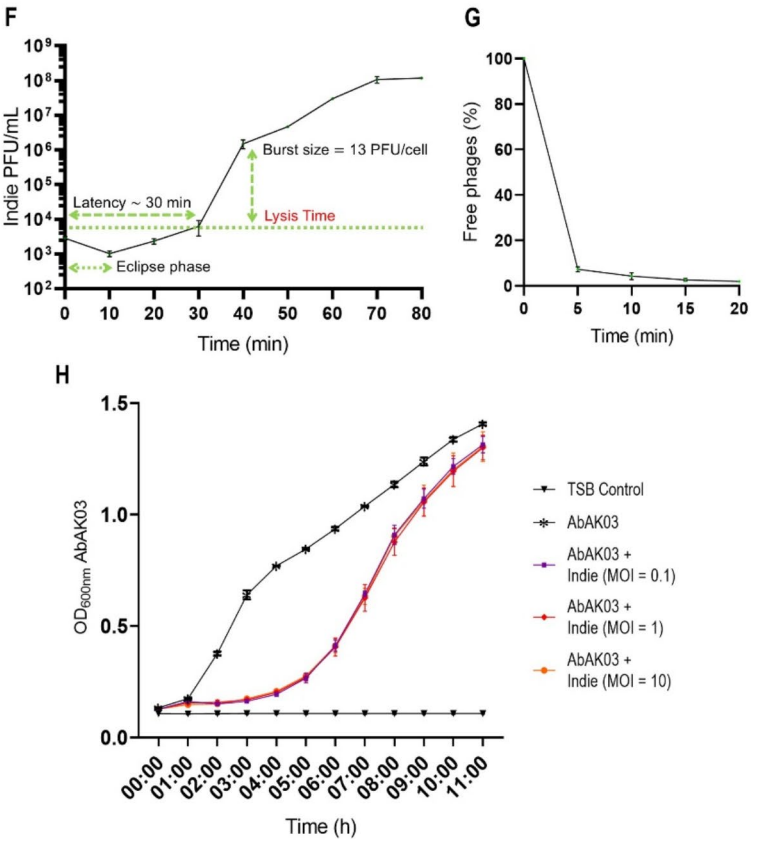

Fig. 1. Characterization of phage Indie as a specific phage for *Acinetobacter baumannii*. (**A**) Plaque morphology of the phage Indie on its host bacterium *A. baumannii* strain AbAK03, showing clear areas of lysis surrounded by translucent halos. (**B**) Morphology of phage Indie observed by Transmission Electron Microscopy (TEM). (**C**) Host range. (**D**) Thermal stability; the means that do not share a letter, differ significantly. (**E**) pH stability; the means that do not share a letter, differ significantly. (**F**) One-step growth curve. (**G**) Adsorption curve. (**H**) Bacteriolytic activity at different multiplicity of infection (MOI = 10, 1, and 0.1). The values are the means of three tests ($n = 3$) ± standard deviation (SD) in all the graphs.

Phage host range and efficiency of plating (EOP)

To understand phage specificity and their ability to infect different bacterial strains, we evaluated 10 clinical strains of *A. baumannii* and other ESKAPE clinical strains and Gram-negative pathogens for the lytic spectrum. Phage Indie formed transparent plaques in two of these *A. baumannii* strains, accounting for 20% (2 of 10), and in one clinical strain of *K. pneumoniae*. The EOP was categorized as high (EOP ≥ 0.5) (Fig. 1C).

Determination of phage stabilities

We conducted tests to evaluate pH and thermal stability to ensure the phage's efficacy under diverse conditions, with the goal of ensuring its reliability for therapeutic applications. pH stability tests revealed that phage Indie remained infectious within the pH range of 2 to 11 but became inactive under alkaline conditions at pH 12 (Fig. 1D). Phage Indie remained stable at 4 °C and retained lytic activity up to 60 °C. However, its activity significantly declined ($P < 0.05$) after 1 h of incubation at 70 °C (Fig. 1E).

Phage adsorption rate, one-step growth curve, and efficiency of bacterial Lysis

The therapeutic efficacy of phage Indie was initially assessed based on its infection parameters. According to the one-step growth curve, the phage exhibited a latent period of 30 min, with an estimated average burst size of 13 PFU/cell (Fig. 1F). The adsorption rate of phage Indie indicated that approximately 95% of the phages adhered to their host within 10 min, demonstrating the speed of phage adsorption (Fig. 1G). We further investigated the lytic activity of phage Indie by exposing *A. baumannii* strain AbAK03 to various phage multiplicities of infection (MOI) (0.1, 1, and 10). As shown in Fig. 1H, the OD_{600nm} values of *A. baumannii* at all MOIs tested were lower than those of the control up to 4 h after a 17-h incubation. Nevertheless, irrespective of the phage MOI, the strains developed resistance to the phage and resumed growth shortly afterward. The repeated measures design indicated that there were no significant differences ($P = 0.116$) in bacterial growth among the different MOIs. The growth curve revealed that even at a low MOI (0.1), growth of *A. baumannii* strain AbAK03 was inhibited for up to 4 h.

Genome analysis

Comprehensive genomic analyses confirmed the safety and therapeutic potential of phage Indie for clinical application (Fig. 2A) because no lysogenic genes were identified in phage's genome, such as integrases, recombinases, repressors, or superinfection immunity proteins. Additionally, comparisons with ABRIcate databases, including NCBI, CARD, ARG-ANNOT, Resfinder, MEGARES, and VFDB, revealed no virulence or antibiotic resistance genes, supporting its safe use against MDR *A. baumannii* clinical strains. PhageAI predicted a virulent lifestyle with a 98.44% probability, classifying it as a lytic phage. Moreover, no transfer RNA (tRNA) genes were identified using tRNAscan-SE.

The genome of phage Indie contains 149 putative ORFs, which are categorized into five modules: DNA metabolism, lysis, structure, packaging, and hypothetical proteins (Fig. 2B). The main characteristics of the predicted ORFs are detailed in Table S1.

Notably, 37 ORFs are hypothetical proteins, while others encode functions related to DNA metabolism, such as DNA polymerase I, helicase, primase, HNH endonuclease, metallo-phosphoesterase, peptidase (ORF 4), right parallel beta-helix repeat-containing protein, RNA polymerase, endonuclease (ORF 15), and exonuclease (ORF 14). Structural protein-coding genes include tail and head proteins, including internal virion proteins A and B. Genome packaging and assembly genes include the small terminase subunit and the large terminase subunit. Additionally, the genome contains genes with lysis functions, such as holin (ORF 82), spanin (ORF 52), endolysin (ORF 24), and an internal virion protein with an endolysin domain (ORF 50).

Phylogenetic analysis and genome comparison of phage Indie

To identify the closest relatives and taxonomic classification of phage Indie, the complete genome underwent nucleotide BLAST® analysis in the GenBank database. That revealed related phages from *Klebsiella*, *E. coli*, *Shigella*, and *Acinetobacter*. To explore their evolutionary relationship, 19 phages within the *Caudoviricetes* class, sharing over 80% nucleotide identity, were selected for phylogenetic analysis. The average nucleotide identity and Blastn-based alignment showed that most phages had over 70% nucleotide sequence coverage, with the closest relative being the *Klebsiella* phage VLCpiA1a (ON602732) (Fig. 2C), sharing 82% sequence coverage and 94.34% identity, situated in the *Drulisvirus* genus within the *Autographiviridae* family.

Intergenomic similarities between viral genomes using VIRIDIC indicated that phage Indie and all 19 phages were above 70%, placing phage Indie within the *Drulisvirus* genus, and represents a new unclassified species within the *Caudoviricetes* class (Fig. 3A). A phylogenetic tree was generated using whole-genome-based analysis, specifically employing the Genome-BLAST distance phylogeny method (Fig. 3B), showing that its closest ancestors are *Klebsiella* phages. Furthermore, PhageAI and the International Committee on Taxonomy of Viruses corroborate the taxonomic classification of phage Indie, assigning it to the *Autographiviridae* family with 97.62% probability and the *Drulisvirus* genus with 99.21% probability.

Enhanced synergy: Bacteriophage Indie augments the efficacy of antibiotics against MDR *Acinetobacter baumannii*

We conducted *in vitro* PAS experiments using the checkerboard method with varying antibiotic concentrations and phage dilutions to understand the impact of combined phage-antibiotic therapy on the bacterial growth of MDR *A. baumannii* strain AbAK03. Bacterial growth was evaluated by OD_{600nm} values and visualized as synograms. These synograms help analyze interactions between phages and antibiotics, highlighting synergies, antagonisms, or additive effects, and clarify how specific combinations influence bacterial viability over time, to identify the most effective dose of phage and antibiotic to be applied in future preclinical trials. The study

A

Phage name	Indie	VLCpiA1a
Genome length (bp)	43,285	43,524
GC content (%)	54.1	54.1
ORFs	149	148
tRNAs	0	0
Antibiotic resistance genes	0	0
Virulence genes	0	0
Lysogeny genes	0	0

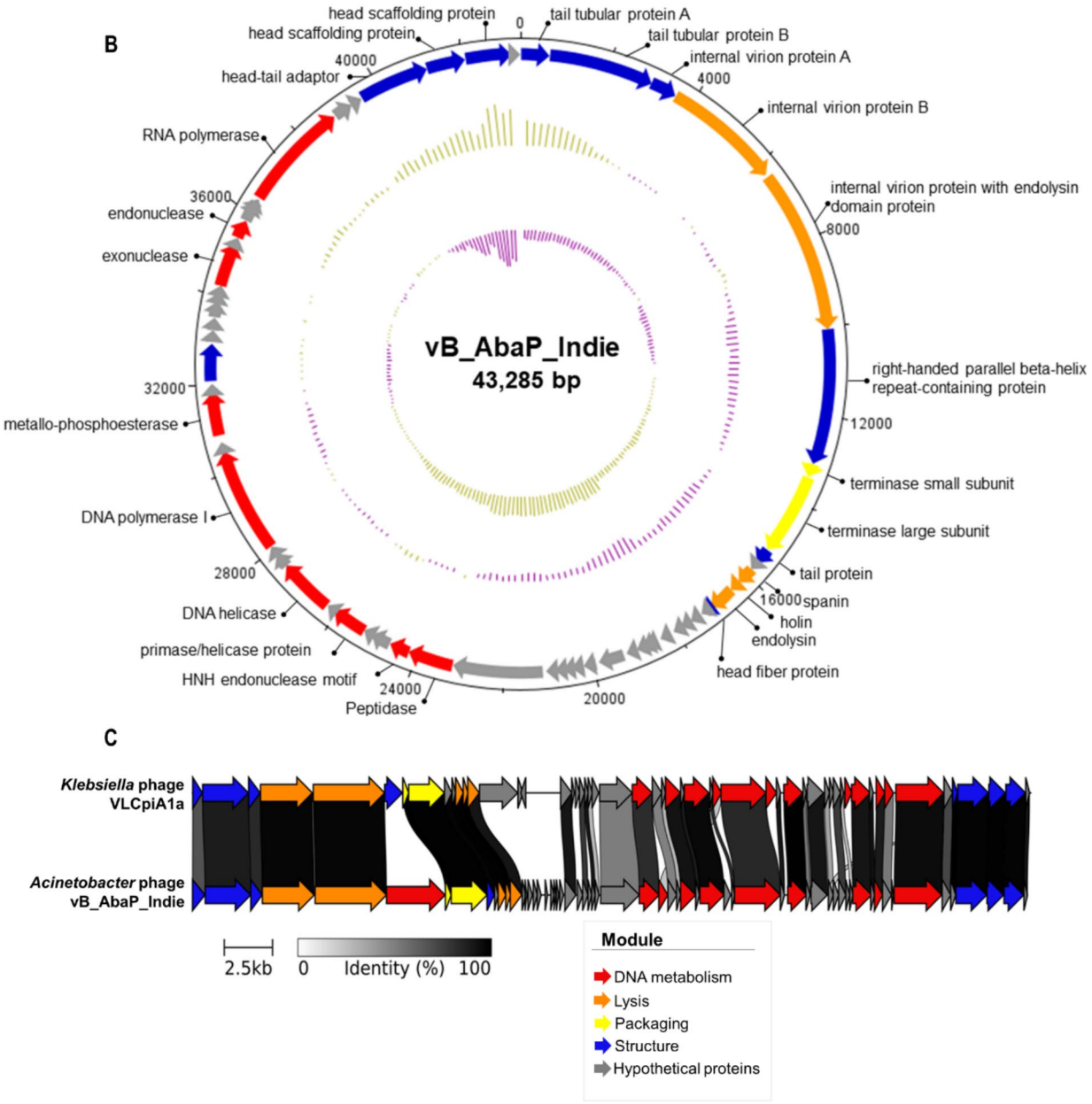

Fig. 2. Genomic analysis of phage Indie belonging to the *Drulisvirus* genus. (**A**) Whole genomic analysis of phage Indie and its closest similar phage VLCpiA1a (ON602732). (**B**) Genome map using DNAPlotter software. (**C**) Comparison of phage Indie and phage VLCpiA1a genomes using Clinker software. In these maps, colored arrows represent the open reading frames (ORFs) according to their functional classification within the respective module. Empty regions indicate the absence of BLAST hits between phage Indie and the genome reference.

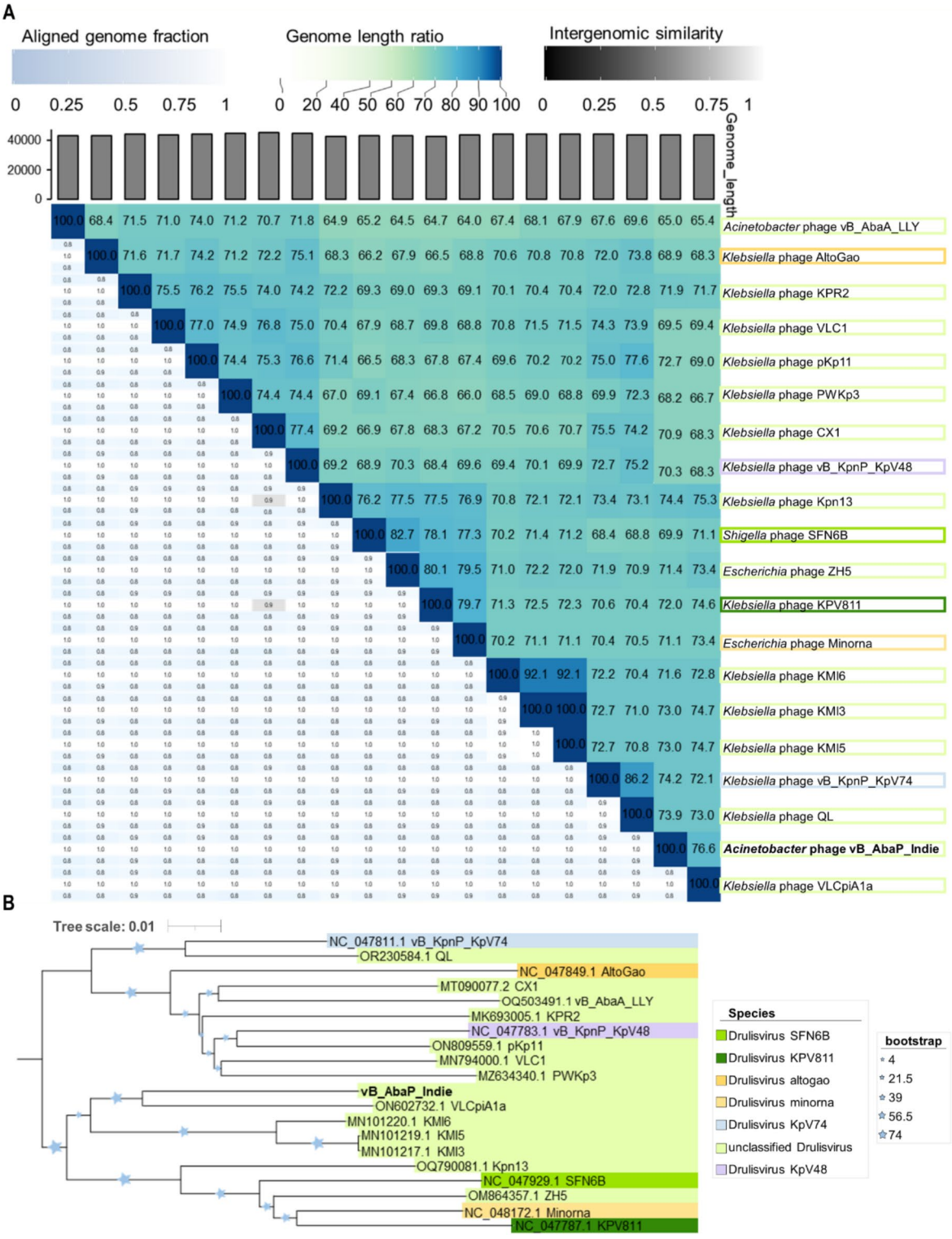

Fig. 3. Phylogenetic and comparative genomic analysis of phage Indie. (**A**) Heatmap of VIRIDIC software. The values of percentage identity range from 0 (0%, white) to 1 (100%, blue). (**B**) Phylogenetic tree of phage Indie based on Genome-BLAST Distance Phylogeny of the *Autographiviridae* family, *Drulisvirus* genus.

measured bacterial population reduction at 17 h (Figs. 4A and 5A) and the percentage reduction of the area under the curve (Figs. 4B and 5B).

The combination of phage Indie and ceftazidime exhibited a strong synergistic effect (Fig. 4C), achieving > 85% elimination of *A. baumannii* strain AbAK03 using lower concentrations of phage (10^5 PFU/mL) and ceftazidime (1.6 µg/mL) within 17 h. This combination yielded a ΣFIC of 0.051, confirming strong synergy based on the

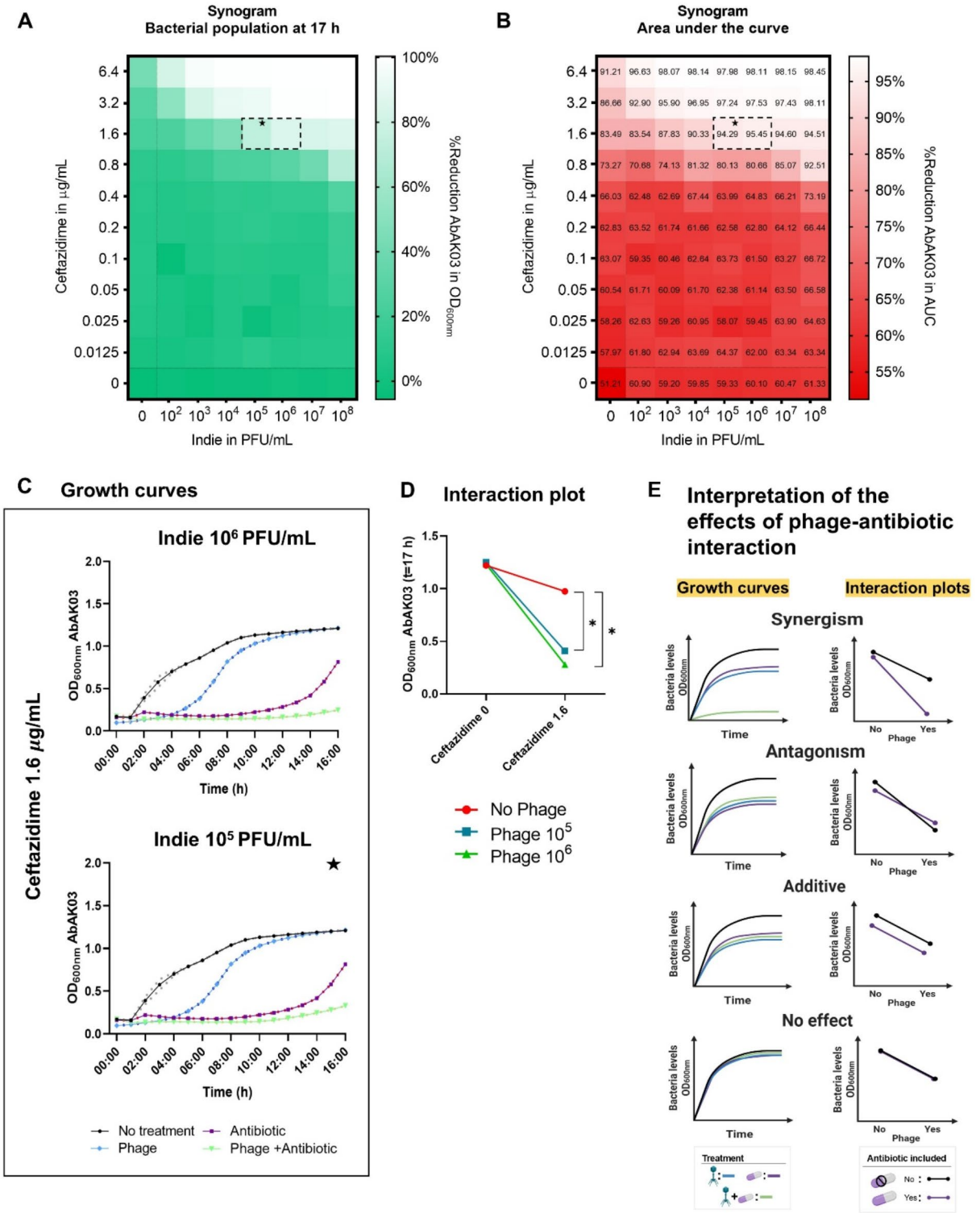

Fig. 4. *In vitro* phage-antibiotic synergy. (**A**) Synogram (t = 17 h) of ceftazidime and phage Indie for reducing bacterial OD_{600nm}. (**B**) Synogram of ceftazidime and phage Indie for the reduction of area under the curve (AUC). Wells below the dotted line contained a single phage treatment. (**C**) Growth curves showing the effect of the phage-antibiotic combination on achieving effective bacterial suppression. (**D**) Interaction plot of ceftazidime and phage Indie. (**E**) Interpretation guide for the effects of the phage-antibiotic combination. Values represent the means of three tests ($n = 3$) ± standard deviation. The two-way ANOVA for statistical analysis in the interaction graphs includes factors: treatment and antibiotic dose, with statistical significance set at * $P = 0.001$.

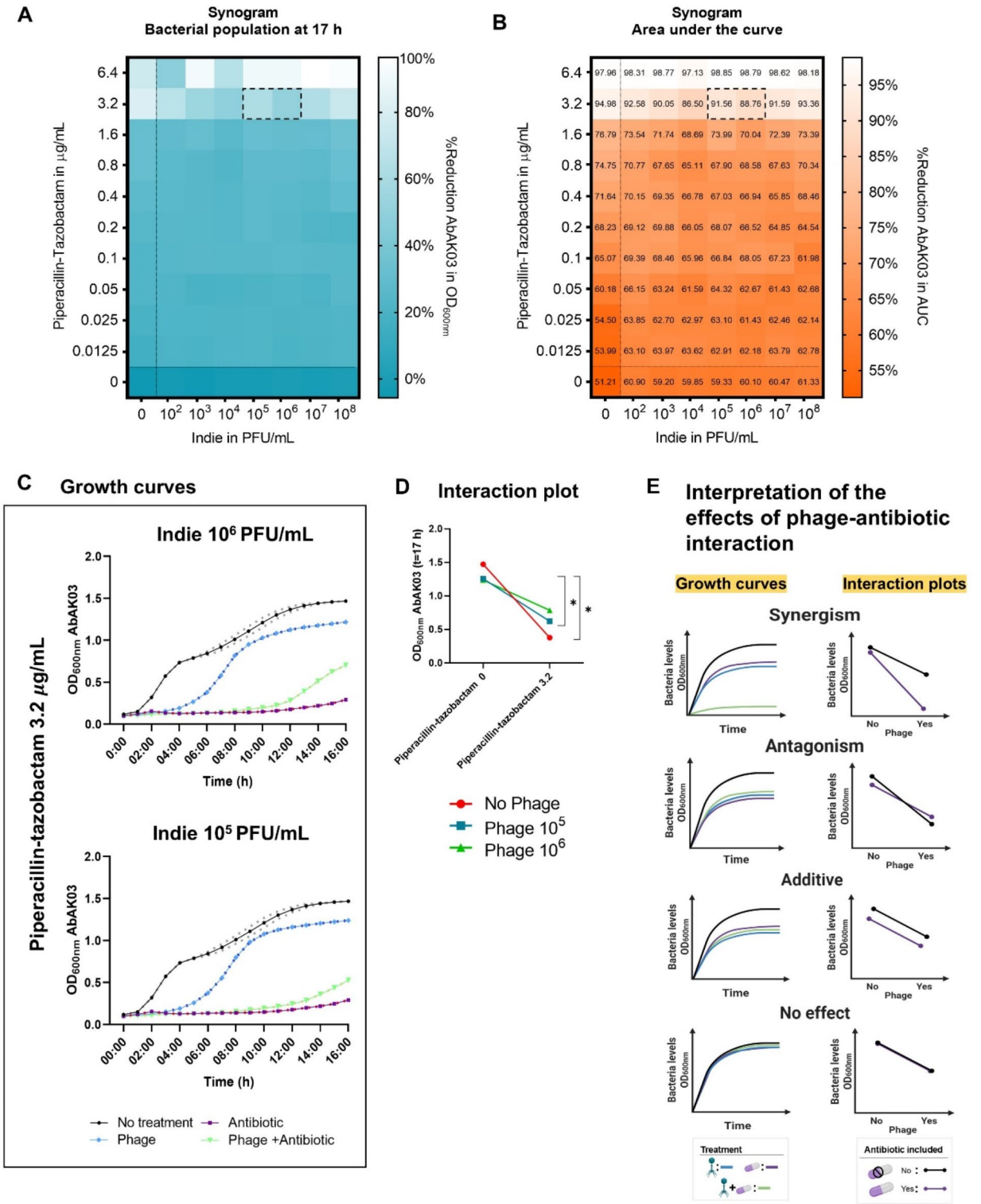

Fig. 5. *In vitro* phage-antibiotic synergy. (**A**) Synogram (t = 17 h) of piperacillin-tazobactam and phage Indie to reduce bacterial OD_{600nm}. (**B**) Synogram of piperacillin-tazobactam and phage Indie to reduce the area under the curve (AUC). Wells below the dotted line contained a single phage treatment. (**C**) Growth curves showing the effect of the phage-antibiotic combination on achieving effective bacterial suppression. (**D**) Interaction plots of TZP and phage Indie. (**E**) Interpretation guide for the effects of the phage-antibiotic combination. Values represent the means of three tests ($n = 3$) ± standard deviation. The two-way ANOVA for statistical analysis in the interaction graphs includes factors: treatment and antibiotic dose, with statistical significance set at $^*P = 0.001$.

standard interpretive threshold (ΣFIC ≤ 0.5). Moreover, the synergy overcame phage resistance within 4 h of *in vitro* treatment, extending bacterial suppression for an additional 13 h, thereby enhancing the bactericidal effect compared to monotherapies. Furthermore, we report that the synergy between phage Indie and ceftazidime allowed the use of significantly lower doses of phage and antibiotics than previously reported in previous studies[30]. The interaction plot (Fig. 4D) compared the final effect of ceftazidime with and without phage. This graph illustrates that the inclusion of phage Indie significantly amplified the bactericidal impact of ceftazidime, surpassing the effects of either the phage or the antibiotic used independently, as demonstrated by the diverging lines in the graphic, concerning the previous interpretation guide (Fig. 4E). Importantly, the synergy of phage Indie and ceftazidime helped to resensitize the *A. baumannii* strain AbAK03 to the antibiotic and producing phage-resistant bacteria that were resensitized to antibiotics for further studies, as indicated by the MIC analysis that revealed its initial resistance.

The combination of phage Indie with piperacillin-tazobactam exhibited an antagonistic effect, reducing *A. baumannii* strain AbAK03 by > 95% within the first 8 h of *in vitro* PAS treatment. Accordingly, the combination of phage Indie (10^5 PFU/mL) and piperacillin-tazobactam (3.2 µg/mL) yielded a ΣFIC of 1.281, indicating partial antagonism according to standard interpretive criteria (ΣFIC > 1.0). However, even with a doubled dose of ceftazidime (piperacillin-tazobactam: 3.2 µg/mL and phage: 10^5 PFU/mL), the outcome was clinically unfavorable, as achieving equivalent bacterial inhibition to MIC would require a higher antibiotic dose, potentially unsafe or unfeasible for patients (Fig. 5C). Furthermore, the interaction plot (Fig. 5D) compared the final effect of piperacillin-tazobactam with and without phage, showing that phage Indie did not enhance the bactericidal effect of piperacillin-tazobactam; instead, it inhibited the impact of phage Indie, as seen in the interpretation guide (Fig. 5E).

The experimental design indicates that the synergistic effect for more significant bactericidal impact in *in vitro* PAS depends on the specific phage and antibiotic tested. Two-way ANOVAs confirmed significant differences between treatments ($P = 0.001$ for ceftazidieme 1.6 µg/mL with phage Indie 10^5 PFU/mL; and $P = 0.001$ for piperacillin-tazobactam 3.2 µg/mL with phage Indie 10^5 PFU/mL). Therefore, the effectiveness of *in vitro* PAS can vary depending on the antibiotic and the specific bacteria being targeted.

Discussion

Phage therapy has emerged as a promising alternative to treat MDR pathogens such as *A. baumannii*[33], recently classified as the most critical nosocomial pathogen[15]. However, implementing these new intervention strategies in clinical settings remains challenging despite the pressing need. This challenge is due to the limited availability of clinically appropriate phages and the lack of detailed characterization, including in-depth genomic analyses and physical stability assessments to ensure their survival during formulation and administration, as well as comprehensive *in vitro* and *in vivo* testing[34].

Here, we have also made progress in translating new intervention strategies by isolating and characterizing a new bacteriophage, phage Indie, which has lytic activity against clinical strains of *A. baumannii*. *In vitro* PAS studies on *A. baumannii* phages are crucial to guide precise *in vivo* experiments and preclinical assays[23,34], as mentioned by Pirnay et al.[35], caution is advised, as some antibiotics may interfere with phage lytic activity.

Therefore, it is essential to evaluate potential synergy or antagonism in phage-antibiotic combinations before clinical application[36], especially since *in vitro* conditions do not fully replicate the host's physiological environment[37,38] and differences in phage-antibiotic pharmacokinetics *in vivo*[30] may influence the therapeutic outcome. Thus, *in vivo* studies are essential to validate the efficacy and clinical applicability of phage Indie against local *A. baumannii* strains.

We demonstrate that phage Indie possesses genetic characteristics that make it suitable for use as a potent and safe antibacterial agent. Notably, it encodes internal virion proteins A and tubular tail B, enhancing adsorption and bacterial synthesis via transmembrane protein binding[39].

The phage also carries lytic enzymes, including holin (ORF 82) for inner membrane permeabilization, spanin (ORF 52) for outer membrane disruption[40], and endolysin (ORFs 24 and 50), which targets peptidoglycan without disrupting the microbiome[38,41]. Additionally, endonuclease and exonuclease (ORFs 15 and 14) facilitate genome segregation, DNA repair, and rRNA maturation[42].

The absence of tRNA genes suggests that the phage fully depends on the host cell's tRNA pool for protein translation[43]. The lack of lysogenic, toxin, or antimicrobial resistance genes supports its therapeutic potential[44].

Specifically, phage Indie represents a new species not classified within the class *Caudoviricetes*, as it shares less than 95% nucleotide identity with known species[31]. This phage belongs to the genus *Drulisvirus* due to > 70% genomic identity[45], with its closest relatives being *Klebsiella* phages, sharing common genomic features[46].

Of note, phage Indie exhibits translucent halos in its plaque morphology, suggesting depolymerase enzyme activity, as reported in *Klebsiella* phages[29,32,47,48]. Similarly, *A. baumannii* phages like vWU2001, Abp95, øFG02, and øCO01 also form plaques with halos, indicating depolymerase presence[29,49,50]. This enzyme facilitates phage adsorption by degrading bacterial exopolysaccharides, which are essential for biofilm formation[51].

On the other hand, phage Indie exhibits a notable degree of specificity, infecting *A. baumannii* and *K. pneumoniae*, two critical pathogens requiring urgent treatment. While broad host range phages can offer versatility in treating mixed infections[52], highly specific phages like phage Indie may be advantageous for targeted therapies, reducing the risk of dysbiosis and off-target effects compared to a narrow host range, which is more specific[53].

For instance, phage Indie was able to lyse 3/15 clinical strains. Other *A. baumannii* phage øCO01 demonstrates a broad host range, infecting 4 out of 10 strains, whereas phages øFG01, øCO02, øCO03, and øLK01 are highly specific, infecting only their respective isolation hosts[49]. Although phages are generally highly specific, often infecting only a single species or serotype[54], this precision allows for targeted bacterial elimination without

disrupting the surrounding microbiota. This characteristic makes them valuable for personalized phage therapy, where specific phages can be selected to effectively treat each outbreak while minimizing unintended effects[22].

This aligns with observations that phages in these natural environments can be specialists, with a narrow host range, or generalists, capable of infecting a broader range of hosts[55]. Some studies have reported wastewater phages capable of infecting multiple bacterial genera[56,57]. However, defining host range is challenging due to variations in testing methods and bacterial defense mechanisms. The terms "narrow" and "broad" are inconsistently used, as most phages are isolated using a single host strain, which may underestimate their true range. Using multiple strains during isolation can reveal broader host ranges, challenging the notion that most phages are highly specific[58].

Despite its specificity, phage Indie represents a promising candidate for treating ESKAPE pathogens-related infections in regional hospitals in Mexico. Its ability to infect selected *A. baumannii* strains, in combination with antibiotics, aligns with the recommendations of Pirnay et al.[35], supporting its potential use in future *in vivo* assays.

Also, it has been previously described that phage intended for clinical use must demonstrate stability to withstand preparation and application, such as in solutions or clinical formulations for patient administration. Phage Indie exhibits thermal and pH survival ranges similar to other reported phages, like the JD419 phage, which shows good stability at pH 6–8 and temperatures from 20 °C to 50 °C[59]. Other phages, such as ZCKp20p remain stable between − 20 °C and 60°C and pH from 2 to 12[60]. This confirms that phage Indie is a suitable candidate for therapy.

Despite its small burst size, comparable to øFG02 with a burst size of 15 PFU/cell and a latency period of 40 min[49], phage Indie's infection process aligns with recent research examining the one-step growth curves of viruses over the last seven decades, revealing burst sizes ranging from 10 to 1000 PFU/cell[61]. The adsorption values are similar to those of other phages[29].

Our data on the bactericidal effect coincide with a recent study[49]; the phage Indie encounters resistance from *A. baumannii* strain AbAK03 after 4 h of activity. We are currently investigating this phenomenon and do not yet have precise data that fully explains the resistance of AbAK03 to the phage. However, previous studies show that phage resistance in *A. baumannii* can arise from alterations in bacterial surface structure[49,62]. Furthermore, the phage-antibiotic synergy, also demonstrated in previous research, supports this approach[28,29,62,63].

It is highlighted that the synergy between phage Indie and ceftazidime, a sublethal dose that alone does not inhibit the growth of *A. baumannii* strain AbAK03, achieved a sustained bacterial reduction of more than 85% for 17 h ($\Sigma FIC = 0.051$). The above reflects the synergistic effect studied in other phages mentioned[24,28,29,62–65], but each phage and MDR strain differ. Hence, based on previous research[36], this study proposes a new phage capable of eradicating ESKAPE pathogens, such as *A. baumannii*. Based on these *in vitro* PAS results, the safety profile of phage Indie is confirmed for its application in an *in vivo* assay in a murine model. This study sheds further light on several issues related to the use of phages in intervention, such as phage and antibiotic selection for designing future controlled clinical trials, phage resistance, and bacteriophage-antibiotic synergy.

Reports suggest that sublethal antibiotic doses can boost phage production by increasing bacterial biomass, accelerating cell lysis, and promoting phage propagation[63]. Additionally, phage-resistant bacteria may lose virulence, increasing their susceptibility to antibiotics[62]. Our *in vitro* results align with the "one-two punch" model[30], where phage Indie partially reduces the AbAK03 population within 4 h, promoting resistant variants that later become resensitized to ceftazidime and eradicated by the phage. It remains necessary to decipher at the phenotypic and genomic levels why there is a more significant bacterial reduction when the phage is combined with one type of antibiotic, while another antibiotic shows no effect or even an antagonistic effect. In this case, both antibiotics are β-lactams, but their sites of action in *A. baumannii* differ ceftazidime targets penicillin-binding proteins (PBPs), while piperacillin, protected by the β-lactamase inhibitor tazobactam, prevents the degradation by bacterial β-lactamases[66].

In conclusion, our findings demonstrate that phage Indie can significantly enhance the eradication of *A. baumannii* in the Sinaloa region of Mexico. This evidence supports the future design of urgently needed controlled *in vivo* trials for compassionate therapy in Mexico and advances research in phage therapy.

Methods

Bacterial strains, characteristics, and growth conditions

Acinetobacter baumannii strain AbAK03 served as the host bacteria for phage Indie, and the phage's host range was tested against nine other *A. baumannii* strains.

The susceptibility of ten *A. baumannii* strains and thirteen ESKAPE pathogens (*E. faecalis*, *S. aureus*, *K. pneumoniae*, and *P. aeruginosa*) and two Gram-negative pathogens (*E. coli*). Strains were obtained from the strain library of the public level three hospital in Culiacan, Sinaloa, Mexico and were grown on tryptose soy agar (TSA) plates (Oxoid Ltd, Hants, UK) at 37 °C for 18 to 24 h.

The identification of clinical strains had been identified by the Vitek®2 (bioMérieux, North Carolina, USA). The bacterial identity of each strain was verified and confirmed by Gram-staining. Moreover, the susceptibility of these bacterial isolates to various traditional antibiotics was examined by measuring the zone of inhibition using the Kirby-Bauer disk diffusion assay as indicated in the manual[67] and interpreted according to the cut-off values specified in the CLSI protocol. The antibiotics used in this study were: ciprofloxacin (CIP), ofloxacin (OFX), norfloxacin (NOR), gentamicin (GM), amikacin (AN), tobramycin (NN), streptomycin (S), aztreonam (ATM), ceftriaxone (CRO), ampicillin-sulbactam (SAM), piperacillin-tazobactam (TZP), cefotaxime (CTX), cefazolin (CZ), vancomycin (VAN), chloramphenicol (C), tetracycline (TE), doxycycline (D), penicillin (P), ampicillin (AM), clindamycin (CC), ceftazidime (CFZ), erythromycin (E), and colistin (CT) (BD Company, USA). The minimum inhibitory concentrations (MIC) of piperacillin-tazobactam and ceftazidime (Sigma-Aldrich, Mexico) for *A. baumannii* were determined using the microbroth dilution method and interpreted following

CLSI protocols. *E. coli* strain ATCC 25922 was used as a positive control for each set of three experimental replicates.

To confirm the identity of the AbAK03 strain, the host bacterium of phage Indie, endpoint polymerase chain reaction (PCR) was conducted. PCR was conducted using pre-designed primers to detect the bla_{OXA-51} gene, as described by Falah et al.[68] for that region (F:5′-TAATGCTTTGATCGGCCTTG-3′ and R:5′-TGGATTGCACT TCATCTTGG-3′). Following PCR, the amplified products were analyzed using 1% agarose gels supplemented with 0.04 µL/mL GelRed nucleic acid stain (Phoenix Research, Candler, NC, USA), and the nucleotide sequences of the amplicons were confirmed through conventional Sanger DNA sequencing (Elim Biopharmaceuticals, Inc., Hayward, CA, USA).

Bacterial strains were cultured in tryptic soy broth (TSB; Oxoid Ltd, Hants, UK) and incubated at 37 °C for 24 h. After incubation, confirmed bacterial stocks were preserved at -80 °C in 20% (v/v) glycerol.

Phage

Phage Indie, used as a model in this study, was obtained from the Laboratorio Nacional para la Investigación en Inocuidad Alimentaria (LANIIA) at the Centro de Investigación en Alimentación y Desarrollo (CIAD), Culiacan unit.

Phage isolation and purification

Phage presence was assessed in wastewater in the influent of the Costa Rica treatment plant, Culiacan, Sinaloa, Mexico, using ten MDR *A. baumannii* strains as the host bacterium. First, wastewater samples were processed immediately after sampling and given pre-treatment for the phage propagation assay as previously described[32]. Subsequently, the samples were treated using a previously described enrichment method[69] with some modifications.

To prepare bacterial cultures, 1 mL of wastewater was combined with 30 mL of double-concentration TSB (Oxoid Ltd, Hants, UK), followed by adding 1 mL of overnight bacterial cultures. The mixture was then incubated at 37 °C for 18 h with gentle agitation at 50 rpm. Then, the samples underwent centrifugation at 8000×g for 10 min at 4 °C using a Megafuge16R (Thermo Fisher Scientific Inc., Waltham, Massachusetts, USA), and the resulting supernatants were filtered through a 0.22 µm pore size nylon membrane (Pall Corp., NY, USA).

Bacteriophages were detected using a spot test employing the double-layer agar method with three replicates. Filtrates were serially diluted, 100 µL of the diluted supernatant was mixed with 1000 µL of an overnight culture of the host bacteria in 3 mL of soft agar (TSB with 0.5% agar), and mixed with host bacterial cultures in soft agar, which were then plated onto TSA plates (Oxoid Ltd, Hants, UK) and incubated at 37 °C for 18 h. Phage plaques were selected based on their clarity.

The bacteriophage was purified using SM buffer (50 mM Tris-Cl, pH 7.5, 100 mM NaCl, 8 mM $MgSO_4 \cdot 7H_2O$) through multiple cycles, at least three times. Purified phages were stored at 4 °C in SM buffer, while stock samples were stored at -80 °C with 20% (v/v) glycerol.

Phage host range and efficiency of plating

The phages' lytic activity was determined against ten *A. baumannii* strains and thirteen ESKAPE pathogens and two Gram-negative pathogens with the spot test as previously described[70] with some modifications. Purified phage suspensions ranging from 10^7 to 10^8 PFU/mL were applied in 10 µL spots onto freshly inoculated bacteria using the double-agar layer method with three replicates. After incubation overnight at 37 °C, a clear area demonstrated the ability of the bacteriophage to lyse.

Depending on this plaque's appearance, the bacteriophages' lytic activity was classified as mentioned[49] with specific alterations: no lysis, phage resistance, partial lysis, nebula lysis, and productive infection. The latter classification of productive infection is characterized by the synthesis in a punctual assay and the formation of plaques on soft agar layer.

Subsequently, to determine the number of viable phages in the total count, the efficiency of plating (EOP) was also performed[43] with three replicates. Thus, all *A. baumannii* strains were cultured overnight (18 h) at 37 °C. For the double-layer agar method, 1000 µL of each overnight culture was combined with 100 µL of diluted phage lysate, prepared in successive dilutions ranging from 10^4 to 10^8 PFU/mL in buffer SM.

The EOP values were determined by dividing the average lysis plaques produced in each susceptible strain by the number of plaques produced on the best host. The strains were categorized based on their EOP values as follows: "high efficiency" ($EOP \geq 0.5$), "medium efficiency" ($0.1 \leq EOP < 0.5$), "low efficiency" ($0.001 < EOP < 0.1$), or "inefficient" ($EOP \leq 0.001$).

Transmission electron microscopy (TEM)

The purified phage suspension was applied onto a copper grid coated with carbon-coated Formvar film and left to sit for 30 min in the dark. It was then negatively stained with 1% phosphotungstic acid for 1 min and air-dried. The sample was subsequently examined using a JEOL 200 CX transmission electron microscope (TEM) (JEOL, Tokyo, Japan) at the Molecular Biology Division of IPICYT (Instituto Potosino de Investigación Científica y Tecnológica A.C.)[71].

Phage thermal and pH stability test

To assess the thermal stability of the bacteriophage, 100 µL of phage was combined with 900 µL of SM buffer adjusted to pH 7.5 and exposed to various temperatures (4 °C, 25 °C, 37 °C, 45 °C, 60 °C, and 70 °C) for 1 h.

Similarly, to evaluate its stability across different pH levels, 100 µL of phage Indie was mixed with 900 µL of SM buffer adjusted to pH levels ranging from 2 to 12 using NaOH or HCl solutions. The mixtures were then incubated at 37 °C for 1 h.

Phage titers were determined using the double-layer agar method, with three replicates per experiment.

One-step growth curve

The one-step growth curve was performed as described by Orozco-Ochoa et al.[43], with three replicates. The burst size was determined as the ratio of the final count of released phage particles to the initial count of infected bacterial cells, divided by the number of infected cells (phage titer at 0 min − phage titer at 0 min with chloroform).

Phage adsorption assay

The adsorption assay was conducted in triplicate as previously described, with minor modifications[72].

Bacteria in exponential growth phase at 10^8 CFU/mL concentrations were centrifuged at 8000×*g* for 10 min and resuspended in TSB. The cell suspension was diluted (10^7 CFU/mL) in 9 mL of fresh TSB. Subsequently, 1 mL of phage was added (MOI = 0.1) and incubated at 37 °C for 5 min.

After 5 min of incubation, the samples were centrifuged at 15,000×*g* for 1 min to collect free unbound phages. This process was repeated every 5 min for a total of 20 min. The percentage of free phages was determined relative to the initial phage concentration at 0 min.

Bacteriolytic activity test

The bacteriolytic activity *in vitro* was evaluated using a 96-well microplate system, following the methodology outlined by Gonzalez-Gomez et al.[73], in triplicate.

An overnight culture of *A. baumannii* strain AbAK03 was adjusted to an OD_{600nm} of 1.5 (~ 10^8 CFU/mL) for inoculation. Phage dilutions were prepared to achieve MOIs values of 10, 1, and 0.1.

The positive control contained 200 µL of *A. baumannii* culture, while the negative control contained only TSB. In the experimental wells, 100 µL of TSB and 80 µL of the phage dilution were added to achieve the desired MOI. After that, 20 µL of the bacterial culture was added to each well, resulting in a final volume of 200 µL per well.

The microplate was then incubated at 37 °C for 17 h in a Synergy HT microplate reader (Biotek, Inc., Winooski, VT, USA), with readings at 600 nm taken every 15 min after orbital shaking before each reading.

Genomic phage DNA extraction and sequencing

The phage genomic DNA extraction was conducted by utilizing the phenol-chloroform method outlined by Sambrook and Russell[74]. In brief, 1 mL of phage suspension was placed into a 1.5 mL microtube and treated with 10 µL of DNase I/RNase A (10 mg/mL) at 37 °C for 30 min. This was followed by the addition of 50 µL SDS (10%), 40 µL EDTA (0.5 M), and 2.5 µL proteinase K (20 mg/mL), and then incubated at 56 °C for 2 h. Equal volume of phenol-chloroform (1:1, v/v) was added, mixed, and centrifuged at 3500×*g* for 10 min. The aqueous layer was transferred, combined with an equal volume of phenol-chloroform (1:1, v/v), and subjected to centrifugation at 3500×*g* for 10 min at 25 °C. This was repeated three more times, where the resulting aqueous layer was combined with 200 µL of 3 M sodium acetate and ethanol, stored at -20 °C overnight, and centrifuged at 15,000×*g* for 30 min. The DNA pellet was washed with 70% ethanol, air-dried, resuspended in 20 µL of nuclease-free water, and stored at -20 °C. DNA quantification was performed using a NanoDrop 2000c spectrometer (Thermo Scientific, Wilmington, USA), and DNA quality was assessed via electrophoresis.

DNA libraries were prepared according to the manufacturer's guidelines using the Nextera XT Library Preparation Kit (Illumina, San Diego, CA, USA). Subsequently, the libraries were quantified using a Qubit 2.0 fluorometer (Thermo Fisher Scientific, Waltham, MA, USA). Genome sequencing was conducted on the Illumina MiniSeq platform at CIAD (Centro de Investigación en Alimentación y Desarrollo) Mazatlan unit, employing a 2 × 150 bp paired-end protocol with 300 cycles. Raw reads were trimmed by fastp v0.23.0[75] and *de novo* assembled was performed using SPAdes v3.15.5[76] with a 10× coverage threshold employed to assemble the contigs.

Bioinformatics analyses

Following the assembly, contigs were annotated in PATRIC v.3.36.16.1 using the phannotate algorithm (https://www.patricbrc.org/app/Annotation). Then, Blastn was employed to compare the complete genome sequence of phage Indie with those stored in the NCBI database, allowing for the identification of phages with the most similar sequences in GenBank, and we selected one as the genome reference. After that, phage Indie was manually curated with its genome reference using Geneious v.9.1.8.

To classify the phage lifestyle, the AI-driven software platform PhageAI v.0.10.0 (https://phage.ai/) was used. Putative transfer RNA (tRNA) encoding genes were predicted using tRNAscan-SE v.2.0[77]. Virulence and antibiotic resistance gene annotation was examined through ABRicate v.0.8.13 (https://github.com/tseemann/abricate). The analysis incorporated the databases NCBI, CARD, ARG-ANNOT, Resfinder, MEGARES, and Virulence Factor Database (VFDB).

Putative open reading frames (ORFs) were annotated using ORF finder (https://www.ncbi.nlm.nih.gov/orffinder/) and the protein was analyzed using the Basic Local Alignment Search Tool (Blastp) available on the NCBI server (https://blast.ncbi.nlm.nih.gov/Blast.cgi), utilizing the Non-Redundant Protein Database. Parameters included a score threshold of > 50 and an e-value threshold of $< 1.0 \times 10^{-3}$. The ORF functions were curated using Artemis Comparison Tool (ACT) v.18.2.0.

For phylogenetic analysis, following alignment, the VICTOR Virus Classification and Tree Building Online Resource (https://ggdc.dsmz.de/victor.php) was utilized to ascertain the phylogenetic relationships. This process involved incorporating phylogenomic trees generated via the Genome-BLAST Distance Phylogeny method. The outputs in Newick format were then employed to construct a phylogenetic tree using iTOL v.6.9.1 (https://itol.

embl.de). The complete phage genome was utilized to compute intergenomic similarities among viral genomes using the VIRIDIC web tool (https://rhea.icbm.uni-oldenburg.de/viridic/), employing default Blastn settings for the alignment.

Furthermore, a global genome map was visualized by DNAPlotter v.18.2.0[78], and the comparison between phage Indie and its genome reference was displayed using clinker v.0.0.28[79].

Phage-antibiotic synergy experiments

The *in vitro* phage-antibiotic synergy (PAS) experiments consist of the methodology previously reported by Gu Liu et al.[36], with minor modifications, using the checkerboard method in triplicate.

Briefly, 100 µL of the overnight culture of *A. baumannii* strain AbAK03 was inoculated into 10 mL of TSB and allowed to grow to the exponential phase (~ 10^8 CFU/mL) at 37 °C with agitation at 50 rpm. The overnight bacterial culture was then adjusted to 10^6 CFU/mL concentration in TSB. Subsequently, 100 µL of this bacterial culture was inoculated into each well of a 96-well microplate containing the phage Indie checkerboard with varying concentrations (50 µL, final 10^2–10^8 PFU/mL) and antibiotic (50 µL, final 0.0125–6.4 µg/mL).

Two β-lactam antibiotics were used for *in vitro* PAS assays: ceftazidime and piperacillin-tazobactam (Sigma-Aldrich, Mexico). Both antibiotics were selected because they are among the leading options used in treating *A. baumannii*[9,25,80,81], in this case, the *A. baumannii* strain AbAK03 is resistant to ceftazidime and is susceptible to piperacillin-tazobactam.

The positive control consisted of *A. baumannii* strain AbAK03 alone, while the negative control contained only TSB. Synergy tests were performed using a Synergy HT microplate reader (Biotek, Inc., Winooski, VT, USA), in which OD_{600nm} was measured every 15 min for a total of 17 h with orbital shaking before of each reading.

Quantification and statistical analysis

Significant differences were analyzed using two-way variance analysis (ANOVA), followed by group comparisons using Tukey's test for the phage thermal and pH stability test.

In the bacteriolytic activity test, a repeated measures design was employed where the nested factor was MOI and the crossed factor was the time, the subject (wells) was nested in the MOI. Also, a comparison between the groups was performed using Tukey's test.

The first step in generating synograms involved normalizing the raw OD data from three biological replicates against the negative control. Interaction plots and two-way ANOVA were utilized to assess the outcomes of each treatment to examine potential synergism between the phage and antibiotic. Interaction plots indicate whether there is an interaction between two separate agents, while the two-way ANOVA test was conducted to determine the statistical significance of the observed visual representations.

The Area Under the Curve (AUC) was performed to quantify the reduction in bacterial levels over time comprehensively. The AUC provides a more complete and accurate measure of the effect of the treatments compared to a single time point. To calculate the percentage reduction in OD or AUC, the following formula proposed by Gu Liu et al.[36]:

$$\text{Reduction } (\%) = \left[\frac{(OD_{\text{growth control}} - OD_{\text{treatment}})}{OD_{\text{growth control}}}\right] \times 100$$

Also, the combination effects of phage-antibiotic were assessed by determining the fractional inhibitory concentration (FIC) index, calculated as previously described Manohar et al.[64]. The effect was evaluated according to the ΣFIC index, classifying it as synergistic ($\Sigma FIC \leq 0.5$), additive ($0.5 < \Sigma FIC \leq 2$), or antagonistic ($\Sigma FIC \geq 2$).

Statistical significance was set at cap $P < 0.05$ for all statistical analyses. Graphing and statistical analyses were performed using Minitab® 19, Minitab Statistical Software (Minitab, LLC.) and GraphPad Prism 8.0.1 (GraphPad Software, Inc., CA, USA).

Data availability

The complete genome sequence of *Acinetobacter baumannii* phage vB_AbaP_Indie has been submitted to the GenBank database and the accession number PQ049254 has been assigned. Data is available from the lead contact upon request.

Received: 2 September 2024; Accepted: 31 March 2025
Published online: 04 April 2025

References

1. Aggarwal, R. et al. Antibiotic resistance: A global crisis, problems and solutions. *Crit. Rev. Microbiol.* **50**, 896–921 (2024).
2. Engeman, E. et al. Synergistic killing and re-sensitization of *Pseudomonas aeruginosa* to antibiotics by phage-antibiotic combination treatment. *Pharmaceuticals (Basel)* **14** (2021).
3. Gulumbe, B. H. et al. Antibiotic resistance and the COVID-19 pandemic: A dual crisis with complex challenges in LMICs. *Health Sci. Rep.* **6**, e1566 (2023).
4. Gordillo Altamirano, F. L. & Barr, J. J. Phage therapy in the postantibiotic era. *Clin. Microbiol. Rev.* **32** (2019).
5. Naghavi, M. Global burden of bacterial antimicrobial resistance 1990–2021: A systematic analysis with forecasts to 2050. *Lancet* **404**, 1199–1226 (2024).
6. OPS/WHO. Antimicrobial resistance puts global health at risk (2021).
7. Santajit, S. & Indrawattana, N. Mechanisms of antimicrobial resistance in ESKAPE pathogens. *Biomed Res. Int.* **2016**, 2475067 (2016).

8. Ahuatzin-Flores, O. E., Torres, E. & Chavez-Bravo, E. *Acinetobacter baumannii*, a multidrug-resistant opportunistic pathogen in new habitats: A systematic review. *Microorganisms* **12** (2024).
9. Shi, J., Cheng, J., Liu, S., Zhu, Y. & Zhu, M. *Acinetobacter baumannii*: An evolving and Cunning opponent. *Front. Microbiol.* **15**, 1332108 (2024).
10. Kon, H., Schwartz, D., Temkin, E., Carmeli, Y. & Lellouche, J. Rapid identification of capsulated *Acinetobacter baumannii* using a density-dependent gradient test. *BMC Microbiol.* **20**, 285 (2020).
11. Akoolo, L., Pires, S., Kim, J. & Parker, D. The capsule of *Acinetobacter baumannii* protects against the innate immune response. *J. Innate Immun.* **14**, 543–554 (2022).
12. Blanco, N. et al. Risk factors and outcomes associated with multidrug-resistant *Acinetobacter baumannii* upon intensive care unit admission. *Antimicrob. Agents Chemother.* **62** (2018).
13. Rocha Lde, A., Vilela, C. A., Cezario, R. C., Almeida, A. B. & Gontijo Filho, P. Ventilator-associated pneumonia in an adult clinical-surgical intensive care unit of a Brazilian university hospital: Incidence, risk factors, etiology, and antibiotic resistance. *Braz. J. Infect. Dis.* **12**, 80–85 (2008).
14. Ye, J. J. et al. Multidrug resistant *Acinetobacter baumannii*: Risk factors for appearance of Imipenem resistant strains on patients formerly with susceptible strains. *PLoS One* **5**, e9947 (2010).
15. WHO. WHO bacterial priority pathogens list. Bacterial pathogens of public health importance to guide research, development and strategies to prevent and control antimicrobial resistance. **72** (2024).
16. CDC. *Antibiotic Resistance Threats [internet]n [internet]he United States [internet]* (U.S. Department of Health and Human Services, CDC, 2019).
17. RHOVE. *Boletín Infecciones Asociadas a la Atención De La Salud [internet]. Vol. Julio-Agosto* (Secretaría De Salud México. Red Hospitalaria de Vigilancia Epidemiológica (RHOVE), 2023).
18. RHOVE-Sinaloa. *Boletin Estatal. Panorama Epidemiológico de las Infecciones Asociadas a la Atención de la Salud* Vol. Diciembre (Secretaría de Salud de Sinaloa, 2023).
19. Suh, G. A., Ferry, T. & Abdel, M. P. Phage therapy as a novel therapeutic for the treatment of bone and joint infections. *Clin. Infect. Dis.* **77**, S407–S415 (2023).
20. Schooley, R. T. et al. Development and use of personalized bacteriophage-based therapeutic cocktails to treat a patient with a disseminated resistant Acinetobacter baumannii infection. *Antimicrob. Agents Chemother.* **61** (2017).
21. Olawade, D. B. et al. Phage therapy: A targeted approach to overcoming antibiotic resistance. *Microb. Pathog.* **197**, 107088 (2024).
22. Palma, M. & Qi, B. Advancing phage therapy: A comprehensive review of the safety, efficacy, and future prospects for the targeted treatment of bacterial infections. *Infect. Dis. Rep.* **16**, 1127–1181 (2024).
23. Zhang, L. et al. Therapeutic evaluation of the *Acinetobacter baumannii* phage Phab24 for clinical use. *Virus Res.* **320**, 198889 (2022).
24. Manohar, P., Loh, B., Nachimuthu, R. & Leptihn, S. Phage-antibiotic combinations to control *Pseudomonas aeruginosa-Candida* two-species biofilms. *Sci. Rep.* **14**, 9354 (2024).
25. Grygorcewicz, B. et al. Environmental phage-based cocktail and antibiotic combination effects on *Acinetobacter baumannii* biofilm in a human urine model. *Microb. Drug Resist.* **27**, 25–35 (2021).
26. Choi, Y. J., Kim, S., Shin, M. & Kim, J. Synergistic antimicrobial effects of phage vB_AbaSi_W9 and antibiotics against *Acinetobacter baumannii* infection. *Antibiotics (Basel)* **13** (2024).
27. Luo, J. et al. Synergy of lytic phage pB23 and meropenem combination against carbapenem-resistant *Acinetobacter baumannii*. *Antimicrob. Agents Chemother.* **68**, e0044824 (2024).
28. Luo, J. et al. Synergistic antibacterial effect of phage pB3074 in combination with antibiotics targeting cell wall against multidrug-resistant *Acinetobacter baumannii* in vitro and ex vivo. *Microbiol. Spectr.* **11**, e0034123 (2023).
29. Wintachai, P. et al. Enhanced antibacterial effect of a novel *Friunavirus* phage vWU2001 in combination with colistin against carbapenem-resistant *Acinetobacter baumannii*. *Sci. Rep.* **12**, 2633 (2022).
30. Gordillo Altamirano, F. L. et al. Phage-antibiotic combination is a superior treatment against *Acinetobacter baumannii* in a preclinical study. *EBioMedicine* **80**, 104045 (2022).
31. Adriaenssens, E. & Brister, J. R. How to name and classify your phage: An informal guide. *Viruses* **9** (2017).
32. Liu, Y. et al. Identification and characterization of capsule depolymerase Dpo48 from *Acinetobacter baumannii* phage IME200. *PeerJ* **7**, e6173 (2019).
33. LaVergne, S. et al. Phage therapy for a multidrug-resistant *Acinetobacter baumannii* craniectomy site infection. *Open. Forum Infect. Dis.* **5**, ofy064 (2018).
34. Delattre, R. et al. Combination of in vivo phage therapy data with in silico model highlights key parameters for pneumonia treatment efficacy. *Cell. Rep.* **39**, 110825 (2022).
35. Pirnay, J. P. et al. Personalized bacteriophage therapy outcomes for 100 consecutive cases: A multicentre, multinational, retrospective observational study. *Nat. Microbiol.* **9**, 1434–1453 (2024).
36. Gu Liu, C. et al. Phage-antibiotic synergy is driven by a unique combination of antibacterial mechanism of action and stoichiometry. *mBio* **11** (2020).
37. Grygorcewicz, B. et al. Antibiotics act with vB_AbaP_AGC01 phage against *Acinetobacter baumannii* in human heat-inactivated plasma blood and *Galleria mellonella* models. *Int. J. Mol. Sci.* **21** (2020).
38. Pekkle Lam, H. Y. et al. Isolation and characterization of bacteriophages with activities against multi-drug-resistant *Acinetobacter nosocomialis* causing bloodstream infection in vivo. *J. Microbiol. Immunol. Infect.* **56**, 1026–1035 (2023).
39. Hu, M., Zhang, H., Gu, D., Ma, Y. & Zhou, X. Identification of a novel bacterial receptor that binds tail tubular proteins and mediates phage infection of *Vibrio parahaemolyticus*. *Emerg. Microbes Infect.* **9**, 855–867 (2020).
40. Liu, M. et al. Comparative genomics of *Acinetobacter baumannii* and therapeutic bacteriophages from a patient undergoing phage therapy. *Nat. Commun.* **13**, 3776 (2022).
41. Kim, K. et al. Characterization of a novel phage PhiAb1656-2 and its endolysin with higher antimicrobial activity against multidrug-resistant *Acinetobacter baumannii*. *Viruses* **13** (2021).
42. Wang, H. et al. Psychrobacter phage encoding an antibiotics resistance gene represents a novel caudoviral family. *Microbiol. Spectr.* **11**, e0533522 (2023).
43. Orozco-Ochoa, A. K. et al. Characterization and genome analysis of six novel *Vibrio parahaemolyticus* phages associated with acute hepatopancreatic necrosis disease (AHPND). *Virus Res.* **323**, 198973 (2023).
44. Lerdsittikul, V. et al. A novel virulent litunavirus phage possesses therapeutic value against multidrug resistant *Pseudomonas aeruginosa*. *Sci. Rep.* **12**, 21193 (2022).
45. Turner, D., Kropinski, A. M. & Adriaenssens, E. M. A roadmap for genome-based phage taxonomy. *Viruses* **13** (2021).
46. Han, P., Pu, M., Li, Y., Fan, H. & Tong, Y. Characterization of bacteriophage BUCT631 lytic for K1 *Klebsiella pneumoniae* and its therapeutic efficacy in *Galleria mellonella* larvae. *Virol. Sin.* **38**, 801–812 (2023).
47. Domingo-Calap, P., Beamud, B., Mora-Quilis, L., Gonzalez-Candelas, F. & Sanjuan, R. Isolation and characterization of two *Klebsiella pneumoniae* phages encoding divergent depolymerases. *Int. J. Mol. Sci.* **21** (2020).
48. Pires, D. P., Oliveira, H., Melo, L. D., Sillankorva, S. & Azeredo, J. Bacteriophage-encoded depolymerases: Their diversity and biotechnological applications. *Appl. Microbiol. Biotechnol.* **100**, 2141–2151 (2016).
49. Gordillo Altamirano, F. et al. Bacteriophage-resistant *Acinetobacter baumannii* are resensitized to antimicrobials. *Nat. Microbiol.* **6**, 157–161 (2021).

50. Huang, L. et al. Characterisation and sequencing of the novel phage Abp95, which is effective against multi-genotypes of carbapenem-resistant *Acinetobacter baumannii*. *Sci. Rep.* **13**, 188 (2023).
51. Vukotic, G. et al. Characterization, antibiofilm, and depolymerizing activity of two phages active on carbapenem-resistant *Acinetobacter baumannii*. *Front. Med. (Lausanne)* **7**, 426 (2020).
52. Fong, K., Wong, C. W. Y., Wang, S. & Delaquis, P. How broad is enough: The host range of bacteriophages and its impact on the agri-food sector. *Phage (New Rochelle)*. **2**, 83–91 (2021).
53. Schmelcher, M. & Loessner, M. J. Application of bacteriophages for detection of foodborne pathogens. *Bacteriophage* **4**, e28137 (2014).
54. Holtappels, D., Alfenas-Zerbini, P. & Koskella, B. Drivers and consequences of bacteriophage host range. *FEMS Microbiol. Rev.* **47** (2023).
55. Myers, J., Ii, D., Lollo, J., Hudec, M. & Hyman, P. G. More's the same-multiple hosts do not select for broader host range phages. *Viruses* **15** (2023).
56. Lopez-Cuevas, O., Castro-Del Campo, N., Leon-Felix, J., Gonzalez-Robles, A. & Chaidez, C. Characterization of bacteriophages with a lytic effect on various *Salmonella* serotypes and *Escherichia coli* O157:H7. *Can. J. Microbiol.* **57**, 1042–1051 (2011).
57. Yildirim, Z., Saksmalli, U. T. & Coban, F. Isolation of lytic bacteriophages infecting *Salmonella* typhimurium and *Salmonella enteritidis*. *Acta Biol. Hung.* **69**, 350–369 (2018).
58. Ross, A., Ward, S. & Hyman, P. More is better: Selecting for broad host range bacteriophages. *Front. Microbiol.* **7**, 1352 (2016).
59. Feng, T. et al. JD419, a *Staphylococcus aureus* phage with a unique morphology and broad host range. *Front. Microbiol.* **12**, 602902 (2021).
60. Zaki, B. M., Fahmy, N. A., Aziz, R. K., Samir, R. & El-Shibiny, A. Characterization and comprehensive genome analysis of novel bacteriophage, vB_Kpn_ZCKp20p, with lytic and anti-biofilm potential against clinical multidrug-resistant *Klebsiella pneumoniae*. *Front. Cell. Infect. Microbiol.* **13**, 1077995 (2023).
61. Jin, T. & Yin, J. Patterns of virus growth across the diversity of life. *Integr. Biol. (Camb)* **13**, 44–59 (2021).
62. Wang, X. et al. Colistin-phage combinations decrease antibiotic resistance in *Acinetobacter baumannii* via changes in envelope architecture. *Emerg. Microbes Infect.* **10**, 2205–2219 (2021).
63. Shlezinger, M., Coppenhagen-Glazer, S., Gelman, D., Beyth, N. & Hazan, R. Eradication of vancomycin-resistant *Enterococci* by combining phage and Vancomycin. *Viruses* **11** (2019).
64. Manohar, P. et al. Synergistic effects of phage-antibiotic combinations against *Citrobacter amalonaticus*. *ACS Infect. Dis.* **8**, 59–65 (2022).
65. Uchiyama, J. et al. Piperacillin and Ceftazidime produce the strongest synergistic phage-antibiotic effect in *Pseudomonas aeruginosa*. *Arch. Virol.* **163**, 1941–1948 (2018).
66. Kyriakidis, I., Vasileiou, E., Pana, Z. D. & Tragiannidis, A. *Acinetobacter baumannii* antibiotic resistance mechanisms. *Pathogens* **10** (2021).
67. CLSI. Performance Standards for Antimicrobial Susceptibility Testing. CLSI Document M100 (Clinical and Laboratory Standards Institute, 2020).
68. Falah, F., Shokoohizadeh, L. & Adabi, M. Molecular identification and genotyping of *Acinetobacter baumannii* isolated from burn patients by PCR and ERIC-PCR. *Scars Burn Heal.* **5**, 2059513119831369 (2019).
69. Gonzalez-Gomez, J. P. et al. Genomic and biological characterization of the novel phages vB_VpaP_AL-1 and vB_VpaS_AL-2 infecting *Vibrio parahaemolyticus* associated with acute hepatopancreatic necrosis disease (AHPND). *Virus Res.* **312**, 198719 (2022).
70. Vashisth, M. et al., Development and evaluation of bacteriophage cocktail to eradicate biofilms formed by an extensively drug-resistant (XDR) *Pseudomonas aeruginosa*. *Viruses* **15** (2023).
71. Yang, Y. et al. A novel *Alteromonas* phage lineage with a broad host range and small burst size. *Microbiol. Spectr.* **10**, e0149922 (2022).
72. Park, D. W. & Park, J. H. Characterization and food application of the novel lytic phage BECP10: Specifically recognizes the O-polysaccharide of *Escherichia coli* O157:H7. *Viruses* **13** (2021).
73. Gonzalez-Gomez, J. P., Rodriguez-Arellano, S. N., Gomez-Gil, B., Vergara-Jimenez, M. J. & Chaidez, C. Genomic and biological characterization of bacteriophages against *Enterobacter cloacae*, a high-priority pathogen. *Virology* **595**, 110100 (2024).
74. Sambrook, J. & Russell, D. W. Extraction of bacteriophage lambda DNA from large-scale cultures using proteinase K and SDS. *CSH Protoc.* (2006).
75. Chen, S., Zhou, Y., Chen, Y. & Gu, J. Fastp: An ultra-fast all-in-one FASTQ preprocessor. *Bioinformatics* **34**, i884–i890 (2018).
76. Bankevich, A. et al. SPAdes: A new genome assembly algorithm and its applications to single-cell sequencing. *J. Comput. Biol.* **19**, 455–477 (2012).
77. Lowe, T. M. & Chan, P. P. tRNAscan-SE On-line: Integrating search and context for analysis of transfer RNA genes. *Nucleic Acids Res.* **44**, W54–W57 (2016).
78. Carver, T., Thomson, N., Bleasby, A., Berriman, M. & Parkhill, J. DNAPlotter: Circular and linear interactive genome visualization. *Bioinformatics* **25**, 119–120 (2009).
79. Gilchrist, C. L. M. & Chooi, Y. H. Clinker & Clustermap.js: Automatic generation of gene cluster comparison figures. *Bioinformatics* **37**, 2473–2475 (2021).
80. Lepak, A. J. et al. Development of modernized *Acinetobacter baumannii* susceptibility test interpretive criteria for recommended antimicrobial agents using pharmacometric approaches. *Antimicrob. Agents Chemother.* **67**, e0145222 (2023).
81. Papazachariou, A. et al. Treatment strategies of colistin resistance *Acinetobacter baumannii* Infections. *Antibiotics (Basel)* **13** (2024).

Acknowledgements

Alma Karen Orozco-Ochoa acknowledges the support received from the Consejo Nacional de Humanidades, Ciencias y Tecnologías (Conahcyt) of Mexico through scholarship [No. 1083340], which finances her doctoral studies. The authors would also like to thank Bertram Lee, Juan Daniel Lira-Morales, José Andrés Medrano-Félix, Célida Isabel Martínez-Rodríguez, and Miriam Vega-Rodríguez for their technical support. Thanks to the Laboratorio Nacional para la Investigación en Inocuidad Alimentaria (LANIIA), Laboratorio Regional de Inocuidad Alimentaria (LARIA) and the Laboratorio de Alimentos Funcionales y Nutracéuticos (LAFN) for providing equipment. We express our gratitude for the contributions of materials from the Instituto Mexicano del Seguro Social Culiacan (IMSS). Additionally, thank you to Araceli Patrón Soberano of the IPICYT (Instituto Potosino de Investigación Científica y Tecnológica A.C.) for technical support in TEM. Certain figures were created using Biorender.

Author contributions

A.K.O.O. performed formal analysis, methodology, and wrote original draft; and J.P.G.G., B.Q., N.C.d., J.B.V.T., and C.C. supervised the investigation, providing further feedback, review and editing. C.C. contributed materials, funding acquisition, validation. All authors read and approved the final manuscript.

Declarations

Competing interests
The authors declare no competing interests.

Additional information
Supplementary Information The online version contains supplementary material available at https://doi.org/10.1038/s41598-025-96669-1.

Correspondence and requests for materials should be addressed to C.C.-Q.

Reprints and permissions information is available at www.nature.com/reprints.

Publisher's note Springer Nature remains neutral with regard to jurisdictional claims in published maps and institutional affiliations.